J. Fluid Mech. (1972), *vol.* 53, *part* 4, *pp.* 759–768
Printed in Great Britain

Effects of the lower boundary on the head of a gravity current

By JOHN E. SIMPSON
Department of Geophysics, University of Reading

(Received 3 September 1971 and in revised form 16 February 1972)

Experimental measurements of the advancing head of a gravity current are described. The head, of depth d in mean cross-section and advancing at mean speed U, has an elevated nose whose mean height h satisfies $h/d = 0{\cdot}61\,Re^{-0{\cdot}23\pm0{\cdot}01}$ through the range $300 \leqslant Re \leqslant 10000$ ($Re = Ud/\nu$). A shifting pattern of lobes and clefts ranges across the head, in which the mean lobe width $\bar{b}$ is found experimentally to satisfy $\bar{b}/d = 7{\cdot}4\,Re^{-0{\cdot}39\pm0{\cdot}02}$. By moving the floor in the direction of the current, or by introducing a thin dense layer beneath it, the lobes and clefts can be suppressed and a purely two-dimensional flow obtained. It is concluded that the lower boundary plays an essential role in determining the substructure of the head and that this originates in convective instability as the head rides over less dense fluid.

1. Introduction

When one liquid flows beneath another whose density is a few per cent less, thus forming a gravity current, there is a complex flow pattern at its leading edge. The lighter liquid, of density ρ and total depth H say, is undercut at velocity U by the gravity current of density $\rho + \Delta\rho$. The current is seen to have an elevated head, which is about twice the height of the following steady flow. At the front of the head an overhang of the denser liquid can be seen. The height h of the nose, the foremost part of this overhang, is only a small fraction of the total height d of the head.

Laboratory fronts, although two-dimensional in their large-scale features, are, when viewed in detail, seen to advance in a series of fairly localized bursts (Ellison 1961). Similar projecting noses with bulges or buttresses which continually change shape have been observed at thunderstorm outflows and sea breeze fronts (Simpson 1969; Lawson 1971) and also in avalanches of powder snow (Seligman 1936).

In the theoretical treatment of the advancing head of a gravity current it is usual to superimpose a velocity U equal and opposite to the forward velocity of the head to bring it to rest. In inviscid liquid theory, which can account for many of the features of such currents, the foremost point S is then seen to be a stagnation point (figure 1). In the theory of von Kármán (1940) and in the extensive treatment by Benjamin (1968) the front is shown to have a slope of $\frac{1}{3}\pi$ at S. A similar result is obtained in the computer-generated profiles of Daly & Pracht (1968).

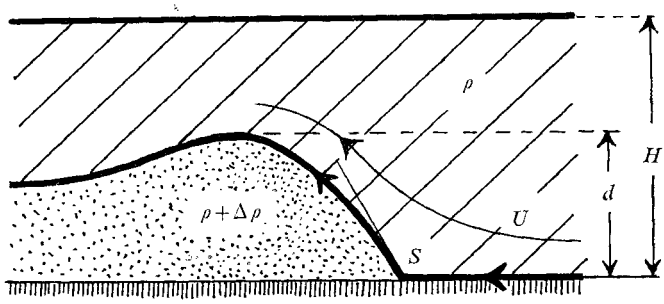

FIGURE 1. Flow relative to gravity current head: inviscid theory. There is no relative motion inside the gravity current head.

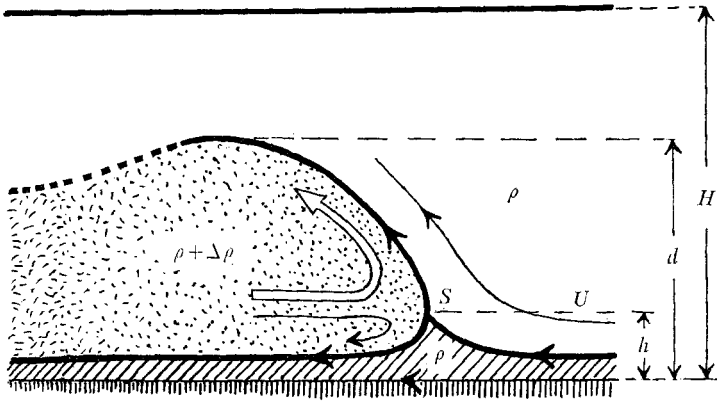

FIGURE 2. Schematic diagram of mean flow relative to a gravity current head subject to no-slip conditions at its lower boundary. /////, liquid which is squeezed beneath the head.

In real flows, with no-slip conditions at the lower boundary due to friction at the stationary ground, the lowest streamlines in the flow relative to the head must be towards the rear. This means that the stagnation point S must be raised some small distance above the floor. In addition to the circulation in the upper part of the head there is a smaller circulation in the reverse sense close to the ground. Using some experimental results of Middleton (1966), Allen (1971) discarded the possibility of a closed streamline loop ahead of S and showed that some of the lighter medium must be squeezed beneath the head. Figure 2 is a schematic diagram of the flow relative to the head in at least some cross-sections.

Close to the floor we have the possibility of gravitational instability. Shifting lobes can be seen in plan at the front and are divided by deep clefts. Their existence makes it clear that the resulting flow (whereby the medium beneath the dividing streamline becomes incorporated into the head) is of a three-dimensional nature.

The shear zone at the upper and rear part of the elevated head is another region where mixing can be seen to occur. Benjamin (1968), by considering the overall balance between horizontal momentum and the hydrostatic pressure gradient, has shown that even idealized gravity currents include a breaking wave, and

Simpson (1969), working with small-scale saline flows, has detected billows resembling those due to Kelvin–Helmholtz instability in this area. The incorporation of the medium beneath the head, dealt with in this paper, involves non-hydrostatic pressure gradients and is seen to disrupt the billows. It thus affects the overall mixing of the head indirectly at the top.

2. Apparatus and procedure

The experiments were carried out in a level Perspex tank, dimensions

$$150 \times 30 \times 30 \text{ cm},$$

divided into two sections by a thin partition 20 cm from one end. By quickly raising the partition the denser liquid was released from this smaller rectangular compartment into the main body of the tank, which contained tap water. The total depth H of the water was 6, 12 or 24 cm. In these conditions the depth d of the mean cross-section of the head of the gravity current is approximately $\frac{1}{2}H$ (Keulegan 1957).

Density differences were obtained by dissolving cooking salt in the lock chamber and ranged from 0·2–6 % by weight of added salt. (1 % of added salt corresponds to 0·76 % actual density difference.) On some occasions sugar was dissolved in both parts of the tank to give increased values of kinematic viscosity up to $3 \times 10^{-2} \text{ cm}^2 \text{ s}^{-1}$.

Measurements involved simple photographic techniques and the following three main viewing and lighting methods were used.

2.1. *Opaque marker*

Milk was mixed with the liquid in the compartment to outline the front of the gravity current. A single photoflood lamp mounted 1 m above the tank illuminated the lobes and clefts forming at the leading edge. This enabled ciné photographs to be taken from the side, from above, or from the front (through the end of the tank).

2.2. *Shadowgraphs*

A 650 W quartz halogen projector lamp, with filament area about 1 cm square, was mounted in a lamp housing 1·5 m above the tank. The sharp density gradients at the leading edge of the current formed clear shadowgraph images on a white screen beneath the tank. Very detailed shadowgraphs were also obtained directly on bromide paper, using for illumination a small electronic flash unit, masked behind an aperture of 3 mm diameter.

To follow lobe elevation in a series of shadowgraphs, the same projector lamp was used, but with its beam interrupted by a shutter. An electric motor rotated a disk 40 cm in diameter with a slit 1 cm wide passing beneath the lamp every $\frac{1}{2}$, 1 or 2 s. This flashing light unit was mounted on a trolley running on rails above the tank. Suspended from the trolley, immediately beneath the tank, was a mask exposing a small section of a long strip of bromide paper. By moving the apparatus along with the head of the current it was possible to obtain a series of non-overlapping shadowgraphs.

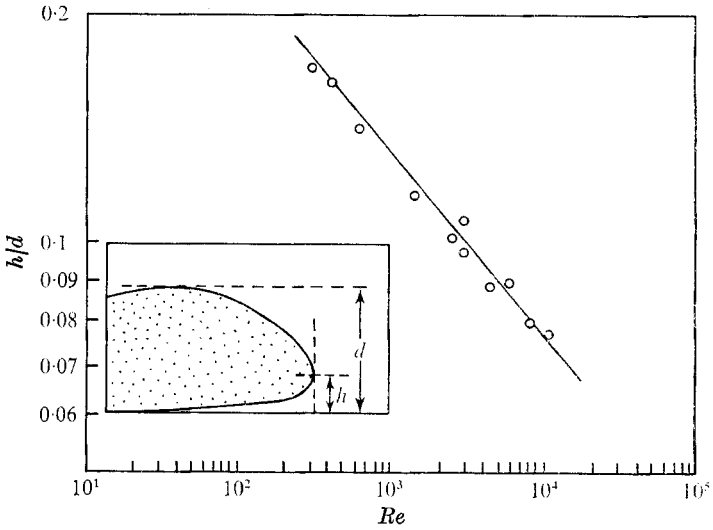

FIGURE 3. Dimensionless nose height h/d plotted against Reynolds number. Ud/ν with log scales.

Measurements were taken directly from bromide paper or from frames of 16 mm film. In the latter case length scales were always included in the photographs.

2.3. *Slit lighting*

Cross-sections of fluorescein-dyed current heads were lit with a narrow beam of light in a vertical plane either along the tank, in the direction of the flow, or across the tank, transverse to the flow. A 500 W quartz halogen lamp, filament length 6 cm, was fitted in a lamp house with a parallel mounted cylindrical lens of dimension 15 × 5 cm. The lamp could be focused to give a beam 1 cm wide in the working area after final masking. The beam was produced either from above or from below and could light a cross-section of up to 30 cm in length.

3. Nose height measurements

Ippen & Harleman (1952), Keulegan (1958), Middleton (1966) and Wood (1965) have suggested a universal shape profile which will approximately fit all gravity current heads of different sizes and velocities. In these profiles, estimates of the dimensionless nose height h/d vary from 0·1 to 0·27. No systematic variation could be detected in these published figures, so a series of measurements was made at different depths d and velocities U.

Using longitudinal slit lighting from beneath the floor of the tank, cross-sections of the nose were filmed from the side with a fixed ciné camera. Profiles were drawn out from ciné frames, using a motion analyser, and a time average of nose heights obtained. A graph of $\log(h/d)$ *vs.* $\log Re$ shown in figure 3 illustrates, through the range $300 \leqslant Re \leqslant 11\,000$ ($Re = Ud/\nu$), the empirical relationship determined by least-squares analysis:

$$h/d = 0{\cdot}61\, Re^{-0{\cdot}23\pm0{\cdot}01} \quad \text{(standard error)}. \tag{1}$$

4. Lobe size measurements

A typical sequence of diagrams showing the development of an advancing front is shown in figure 4. Small ripples form beneath the lower surface of a large advancing lobe; some of these then move to the side and are absorbed in the cleft there. One large cleft continues to develop and a billow is formed at the steepening upright surface behind it, growing into a Kelvin–Helmholtz wave. The extent of the penetration of unmixed fluid in the cleft is of the same order as the lobe size. This is shown in figure 5, which depicts the results of running a gravity current towards the camera through slit lighting transverse to the flow. These surface contours are spaced at horizontal intervals of 2 cm. As well as showing the depth of the clefts, the figure shows the position of the transverse waves forming higher up in the head.

Photographs shown in figures 6(*a*) and (*b*) (plate 1) were taken with similar slit lighting to that used in the nose height measurements, but with fluorescein in the light liquid and no dye in the saline flow. They confirm the depth of indentation of the clefts and also show patches of light liquid trapped beneath the head rising from the floor and being swept towards the nose.

To investigate any relationship between the mean lobe width and Reynolds number Ud/ν the apparatus described in §2.2 was used to make intermittent shadowgraphs of lobe formation. Figure 7 (plate 2) shows part of a record obtained from such a run. From each run a tracing was made of the successive indented leading edges and, as in figure 8, dotted lines were drawn to show the continuity of all the clefts. It can be seen that the clefts are continually absorbed by neighbours, and fresh ones appear by subdivision of large lobes at the points marked with a cross.

When these cleft-continuity lines had been drawn, the widths b of the lobes in each shadowgraph were measured by projecting them onto the tangent to the two foremost lobes. An overall mean $\bar{b}$ was calculated for the set of shadowgraphs corresponding to each Reynolds number. The mean velocity U was found to be constant during each run.

Figure 9 shows a graph of $\log \bar{b}/d$ *vs.* $\log Re$, for Reynolds numbers from 280 to 11200. This indicates an empirical relationship

$$\bar{b}/d = 7{\cdot}4\, Re^{-0{\cdot}39\pm0{\cdot}02} \quad \text{(standard error)}. \tag{2}$$

In addition, for each run all the lobe sizes immediately before subdivision (immediately before a cross) were measured. These were denoted by $b_{\max}$, and the mean of these, $\bar{b}_{\max}$, was also determined. A graph of $\log (\bar{b}_{\max}/d)$ *vs.* $\log Re$ is also shown in figure 9. It has the equation

$$\bar{b}_{\max}/d = 12{\cdot}6\, Re^{-0{\cdot}38\pm0{\cdot}02} \quad \text{(standard error)}.$$

If we combine the result (2) with that given above for mean nose height, equation (1), we see that the ratio of the lobe width to the nose height, $\bar{b}/h$, is weakly dependent on Reynolds number, i.e.

$$\bar{b}/h = 12\, Re^{-0{\cdot}16\pm0{\cdot}02}. \tag{3}$$

As Re increases from 300 to 10000 the ratio $\bar{b}/h$ decreases from 4·8 to 2·7.

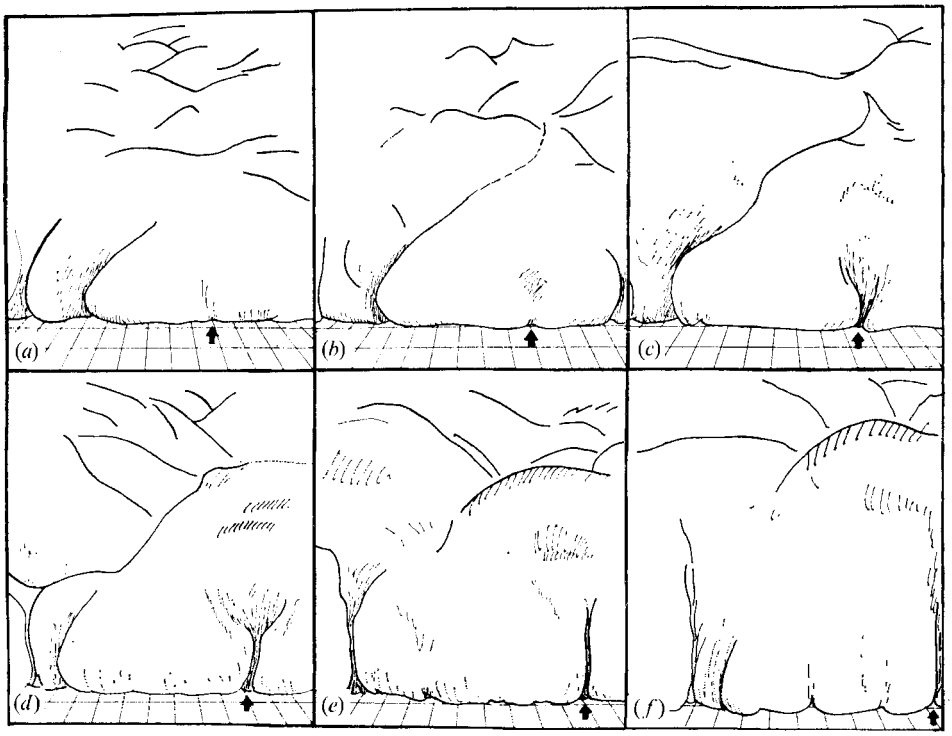

FIGURE 4. Lobe breakdown and cleft formation at an advancing gravity current head.

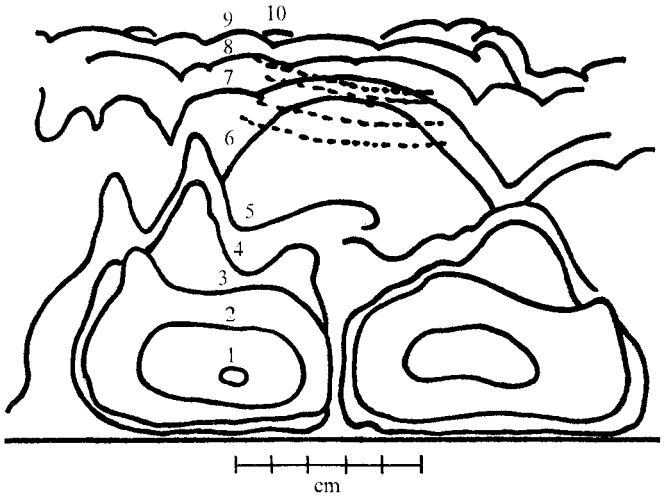

FIGURE 5. Front view of lobe and cleft structure at gravity current head. – – –, position of wave within the head. Horizontal spacing of contours is 2 cm. $\Delta\rho/\rho = 1\,\%$, $H = 24$ cm.

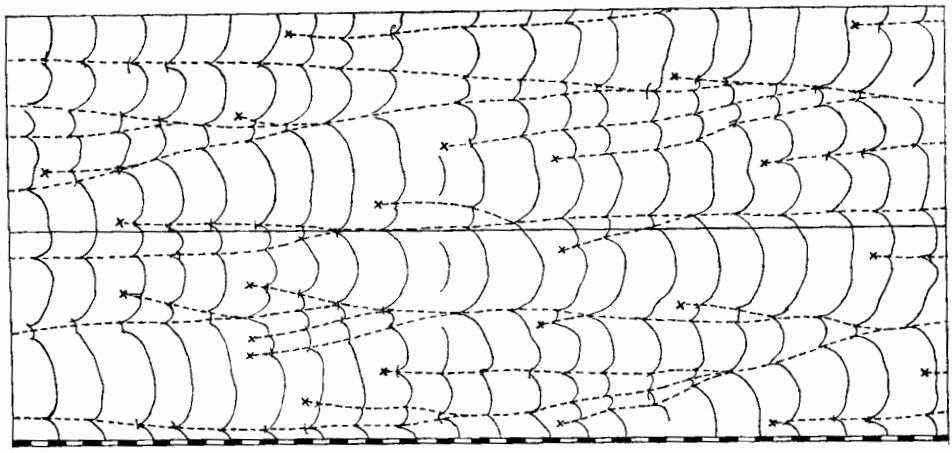

FIGURE 8. Drawing from shadowgraph series showing evolution of lobes. – – –, continuity of clefts; ×, points where new clefts appear. Time interval is 0·5 s, scale in cm, $\Delta\rho/\rho = 1\,\%$, $H = 24$ cm.

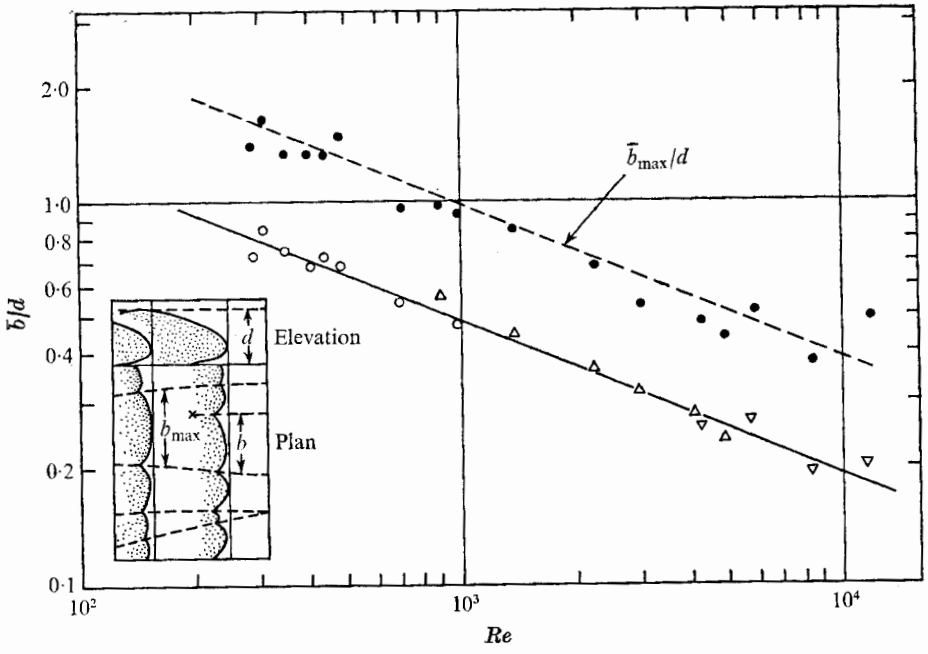

FIGURE 9. Mean dimensionless lobe size plotted against Reynolds number Ud/ν. $\bar{b}_{max}/d$ is also shown. Depth of tank H: ○, 6 cm; △, 12 cm; ▽, 24 cm. $d \doteq \frac{1}{2}H$.

Parameter	$\Delta\rho/\rho$	H (cm)	U (cm s^{-1})	ν (cm^2 s^{-1})	Re (= Ud/ν)	$\bar{b}/d$	h/d
Least value	0·2 %	6	1·11	0·01	280	0·20	0·077
Greatest value	6·0 %	24	10·28	0·03	11200	0·83	0·168

TABLE 1

Table 1 gives the ranges of the parameters involved in the above experimental measurements.

5. Two-dimensional flow

Two methods were found to be effective in reducing or suppressing lobe formation. These produced, for short periods at least, an approximately two-dimensional flow. The first method consisted of reducing the effect of viscous stress due to the floor by moving it in the direction of the current. In the second the layer of potentially unstable liquid beneath the head was eliminated by establishing a thin heavy layer close to the floor before the flow was started.

5.1. *Moving floor*

Profiles of the head were modified by using a thin false floor of Perspex 1 mm thick lying on the floor of the tank, being the same width as the tank, and a third of its whole length. Thin nylon cord attached at one side of the chamfered leading edge was led under a pulley at the end of the tank and wound onto a drum driven by a variable-speed electric motor. The floor was drawn along in the same direction as the gravity current, with its leading edge a few centimetres ahead of the front. For a given water depth and density difference, runs were made at constant floor speed which was increased in successive runs by 1 cm s^{-1}.

For profile examination the lighting and ciné camera were arranged exactly as for the nose height measurements. The effect on the profile of increasing floor speed was to make it progressively flatter. Figure 10 shows this effect in a flow where d was 6 cm and the normal value of U was 4 cm s^{-1}. The nose was nearly on the ground at a floor speed of 4·5 cm s^{-1}, and the lower two thirds of the profile was linear, making an angle with the ground of about $\frac{1}{8}\pi$. The billows at the upper surface of the head became more regular, extending right across the tank at times.

The head, viewed with shadowgraph lighting, was seen to be much less divided into lobes as the speed of the floor approached the speed of the head. At floor speeds a little in excess of the normal speed no lobe pattern could be detected.

If the floor was suddenly brought to rest, a nose formed once more and immediately broke up into a regular series of lobes, indicating the existence of an initially preferred lobe size. This regular pattern then quickly developed into the normal shifting pattern of lobes and clefts. Figure 11 is a tracing from a film showing this effect and figures 12 (*a*), (*b*) and (*c*) (plate 3) contrast the plan view of the three types of leading edge of a gravity current. In figure 12 (*a*) the floor moves at about head speed; there are no lobes, the raised nose has disappeared and a

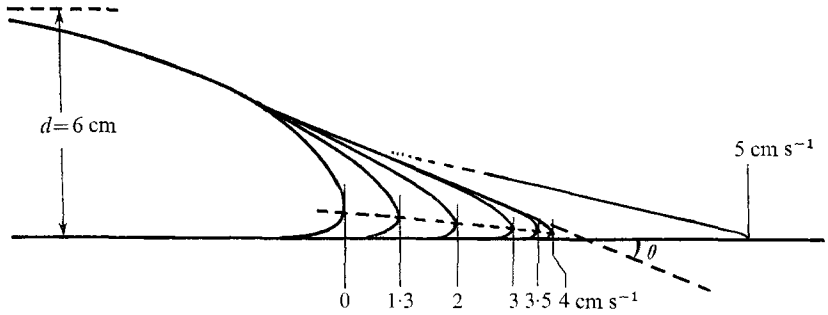

FIGURE 10. Modification of the profile of a gravity current head by moving the floor in the direction of the current. The figures show the speed of the floor. $\Delta\rho/\rho = 1\%$, $H = 12$ cm.

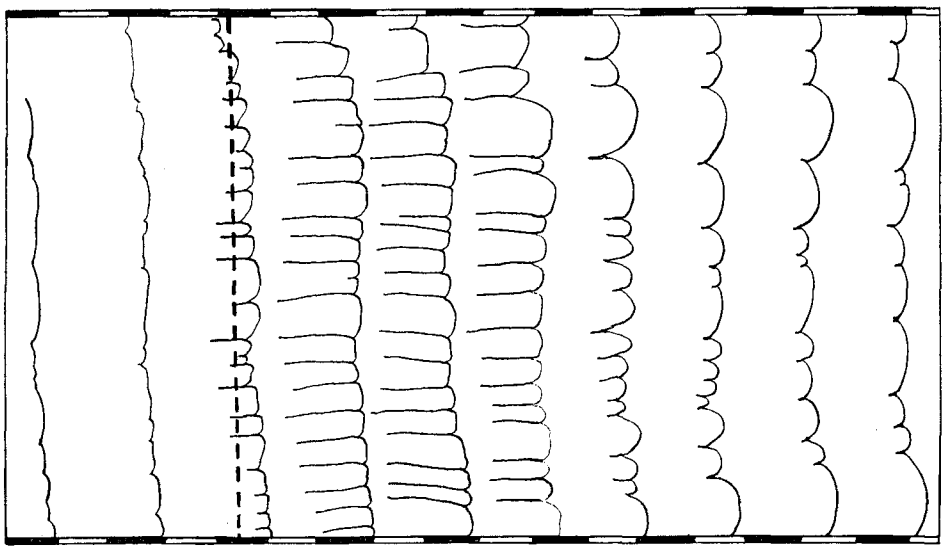

FIGURE 11. Initiation of lobe structure at head of gravity current when a moving floor is brought to rest (at dotted line). Plan view at intervals of $\frac{1}{3}$ s. $\Delta\rho/\rho = 2\%$, $H = 12$ cm, scale in cm.

large roll has formed. In figure 12(*b*) the floor has been brought suddenly to rest; some overhang now exists and a series of filamentary clefts has formed. Figure 12(*c*) shows a normal pattern of lobes and clefts.

5.2. *Heavy layer*

A layer of salt solution on the floor can sometimes inhibit lobe formation and give rise to a truely two-dimensional flow, with tightly rolling-up billows extending right across the tank. Figure 13 (plate 4) shows this effect. No special slit lighting was used to obtain this photograph, which was lit by a single electronic flash 100 cm directly above the head. The width of the tank was 10 cm and the water depth $H = 6$ cm.

In one series of experiments a thin layer of dyed saline solution, of density greater than that of the gravity current, was allowed to spread slowly across the

floor from a dropping funnel at the centre of the tank. After 30 minutes this layer was uniform, and the gravity current was released. With $\Delta\rho/\rho = 0{\cdot}5\ \%$ in the gravity current and twice this in the saline layer, a head of height 12 cm had its lobes suppressed by a layer 3 mm deep. Viewed with slit lighting, the head was seen from the side to ride forward on top of the dye. A little of the dye passed up and over the head, but no signs of lifting dye were visible beneath it.

In another series, the dense layer was spread slowly from the lock end. When sufficient had been introduced to cover the first half of the floor the gravity current was released. While the front was running above the dense layer it was smooth and lobe-free. As it moved forward past the end of the layer, the leading edge became sharply incised, indicating a preferred lobe size. This regular pattern quickly broke down into the usual jumble of lobes and clefts.

6. Conclusion

This experimental work shows that the lobe and cleft structure at the head of a gravity current arises from convective instability produced by light liquid which has been overrun by the denser liquid of the gravity current. The lower boundary layer within the head controls the detailed form of the structure, and an empirical dependence of nose height and of lobe size on Reynolds number for the whole flow is established. Understanding of the nature and quantity of the mixing beneath the nose may have important applications both in meteorological work on cold outflows in the atmosphere and in sedimentology in explaining how slumping flows may be maintained as turbidity currents.

This work was done under a research grant from the Natural Environment Research Council, and I am also indebted to colleagues for many helpful discussions.

REFERENCES

Allen, J. R. L. 1971 *J. Sedimentary Petrology*, **41**, 97.

Benjamin, T. B. 1968 *J. Fluid Mech.* **31**, 209.

Daly, B. J. & Pracht, W. E. 1968 *Phys. Fluids*, **11**, 15.

Ellison, T. H. 1961 *Science Progress*, **49**, 57.

Ippen, A. T. & Harleman, D. R. F. 1952 *Proc. N.B.S. Symp. on Gravity Waves, Nat. Bur. Stand. Circ.* **521**, 79.

Kármán, T. von 1940 *Bull. Am. Math. Soc.* **46**, 615.

Keulegan, G. H. 1957 *U.S. Nat. Bur. Standards Rep.* no. 5168.

Keulegan, G. H. 1958 *U.S. Nat. Bur. Standards Rep.* no. 5831.

Lawson, T. J. 1971 *Weather*, **26**, 105.

Middleton, G. V. 1966 *Can. J. Earth Sci.* **3**, 523.

Seligman, G. 1936 *Snow Structure and Ski Fields*, figure 356. Macmillan.

Simpson, J. E. 1969 *Quart. J. Roy. Met. Soc.* **95**, 758.

Wood, I. R. 1965 *University N.S. Wales. Water Res. Lab., Manly Vale Rep.* no. 81.

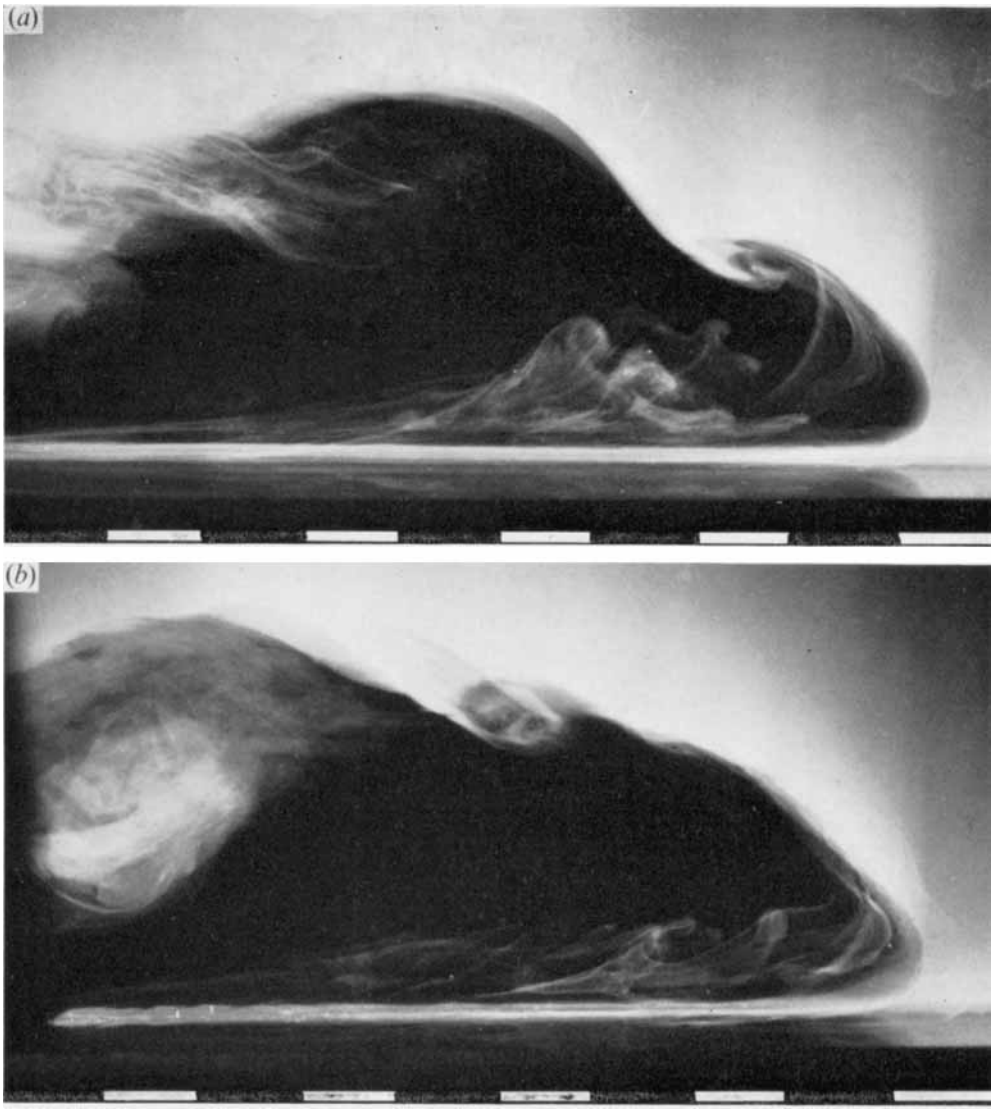

FIGURE 6. Sections of gravity current heads running into a medium dyed with fluorescein. Vertical slit lighting from beneath shows dyed liquid rising from the floor and drawn into clefts. Scale is in cm, $\Delta\rho/\rho = 1\,\%$, $H = 8$ cm.

(*Facing p.* 768)

FIGURE 7. Part of a series of lobe shadowgraphs. $\Delta\rho/\rho = \frac{1}{2}\%$, $H = 24$ cm. Reproduced $\frac{7}{8}$ full-size.

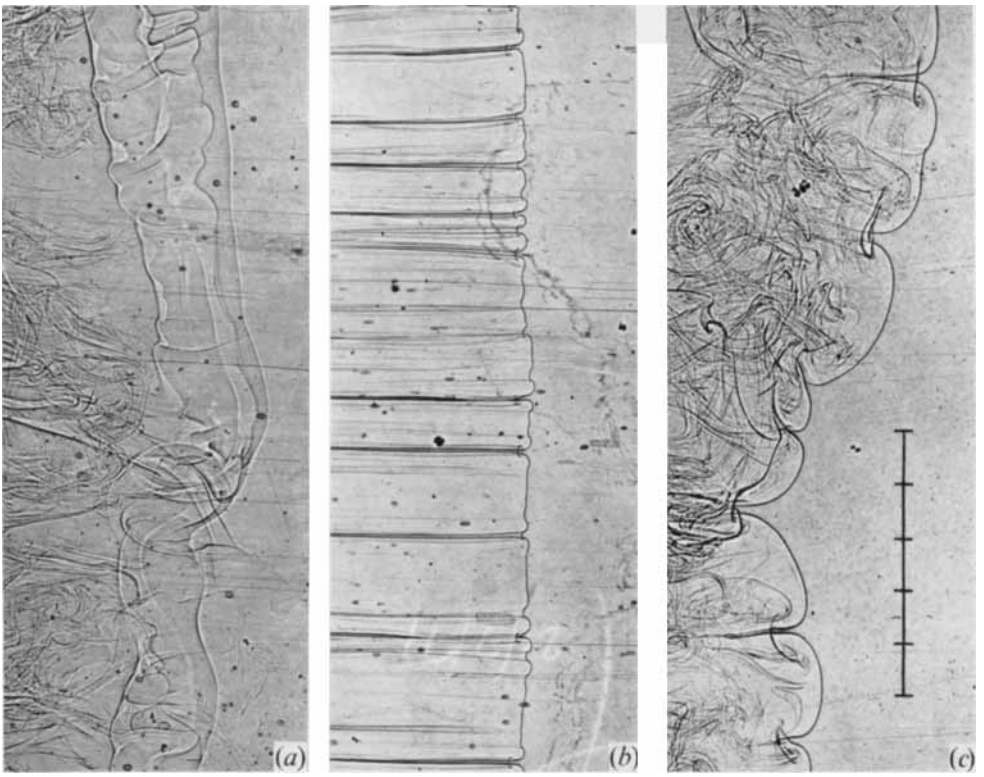

FIGURE 12. Shadowgraphs showing plan view of leading edge of gravity current under different floor conditions. $\Delta\rho/\rho = 1\%$, $H = 12$ cm, scale in cm. (*a*) Floor moving at about head speed. (*b*) Floor suddenly brought to rest. (*c*) Floor fixed; normal pattern of lobes and clefts.

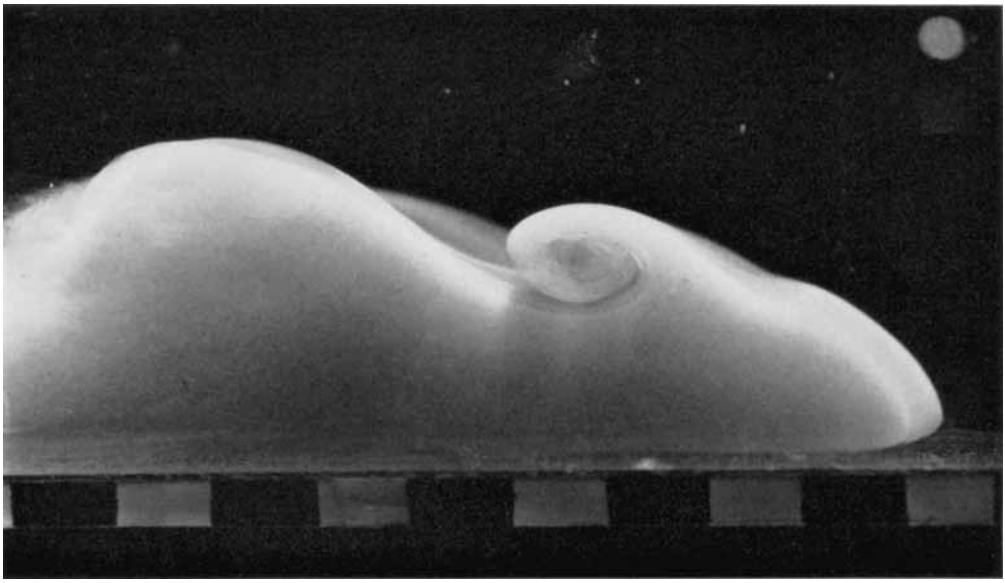

FIGURE 13. A two-dimensional gravity current head moving above a thin saline layer. $H = 6$ cm, $\Delta\rho/\rho = 1\%$, scale in cm.